Journal of Magnetic Resonance 309 (2019) 106615

Contents lists available at ScienceDirect

Journal of Magnetic Resonance

journal homepage: www.elsevier.com/locate/jmr

Exploiting heterogeneous time scale of dynamics to enhance 2D HETCOR solid-state NMR sensitivity

Rongchun Zhang [a,1], Yusuke Nishiyama [b,c,*], Ayyalusamy Ramamoorthy [a,*]

[a] Biophysics and Department of Chemistry, Biomedical Engineering, Maromolecular Science and Engineering, University of Michigan, Ann Arbor, MI 48109-1055, USA
[b] NMR Science and Development Division, RIKEN SPring-8 Center, Nanocrystallography Unit, RIKEN-JEOL Collaboration Center, RIKEN, Yokohama, Kanagawa 230-0045, Japan
[c] JEOL RESONANCE Inc., Musashino, Akishima, Tokyo 196-8558, Japan

ARTICLE INFO

Article history:
Received 26 June 2019
Revised 11 September 2019
Accepted 3 October 2019
Available online 14 October 2019

Keywords:
Solid-state NMR
Cross polarization
NOE
INEPT
Multiphase solids
HETCOR
Signal enhancement

ABSTRACT

Multidimensional solid-state NMR spectroscopy plays a significant role in offering atomic-level insights into molecular systems. In particular, heteronuclear chemical shift correlation (HETCOR) experiments could provide local chemical and structural information in terms of spatial heteronuclear proximity and through-bond connectivity. In solid state, the transfer of magnetization between heteronuclei, a key step in HETCOR experiments, is usually achieved using cross-polarization (CP) or insensitive nuclei enhanced by polarization transfer (INEPT) depending on the sample characteristics and magic-angle-spinning (MAS) frequency. But, for a multiphase system constituting molecular components that differ in their time scales of mobilities, CP efficiency is pretty low for mobile components because of the averaging of heteronuclear dipolar couplings whereas INEPT is inefficient for immobile components due to the short T_2 and can yield through-space connectivity due to strong proton spin diffusion for immobile components especially under moderate spinning speeds. Herein, in this study we present two 2D pulse sequences that enable the sequential acquisition of $^{13}C/^{1}H$ HETCOR NMR spectra for the rigid and mobile components by taking full advantage of the abundant proton magnetization in a single experiment with barely increasing the overall experimental time. In particular, the ^{13}C-detected HETCOR experiment could be applied under slow MAS conditions, where a multiple-pulse sequence is typically employed to enhance ^{1}H spectral resolution in the indirect dimension. In contrast, the ^{1}H-detected HETCOR experiment should be applied under ultrafast MAS, where CP and heteronuclear nuclear Overhauser effect (NOE) polarization transfer are combined to enhance ^{13}C signal intensities for mobile components. These pulse sequences are experimentally demonstrated on two model systems to obtain 2D $^{13}C/^{1}H$ chemical shift correlation spectra of rigid and mobile components independently and separately. These pulse sequences can be used for dynamics based spectral editing and resonance assignments. Therefore, we believe the proposed 2D HETCOR NMR pulse sequences will be beneficial for the structural studies of heterogeneous systems containing molecular components that differ in their time scale of motions for understanding the interplay of structures and properties.

1. Introduction

Solid-state NMR spectroscopy is a powerful analytical tool that is widely used for studying molecular structures and dynamics of a variety of solids including membrane proteins [1–5], multiphase polymers [6–9], bone materials [10–12], amyloids [13–18], and nanocomposites [19–22]. The benefits of multidimensional NMR techniques to obtain higher resolution and higher degree of structural and dynamic information have been well utilized in numerous applications, among which 2D homonuclear (HOMCOR) [23–26] and heteronuclear (HETCOR) [27–32] chemical shift correlation experiments are most widely employed and have become indispensable for structural studies of proteins [33–40].

With the rapid development of ultrafast magic-angle-spinning (MAS) probe technology, ^{1}H spectral resolution can be dramatically enhanced due to efficient suppression of ^{1}H-^{1}H dipolar couplings [41,42], which allow for $^{1}H/^{1}H$ chemical shift correlation [43,44] to probe the proximities of proton atoms in solids. Most

* Corresponding authors at: NMR Science and Development Division, RIKEN SPring-8 Center, Nanocrystallography Unit, RIKEN-JEOL Collaboration Center, RIKEN, Yokohama, Kanagawa 230-0045, Japan (Y. Nishiyama). Biophysics and Department of Chemistry, Biomedical Engineering, Maromolecular Science and Engineering, University of Michigan, Ann Arbor, MI 48109-1055, USA (A. Ramamoorthy).

E-mail addresses: yunishiy@jeol.co.jp (Y. Nishiyama), ramamoor@umich.edu (A. Ramamoorthy).

[1] Present address: South China Advanced Institute for Soft Matter Science and Technology, School of Molecular Science and Engineering, South China University of Technology, Guangzhou 510640, PR China.

https://doi.org/10.1016/j.jmr.2019.106615
1090-7807/

importantly, proton-detection under ultrafast MAS conditions is employed to remarkably improve the signal-to-noise (S/N) ratio of multidimensional experiments [45–53]. In these experiments involving low-γ nuclei, cross polarization (CP) [54,55] is generally employed to enhance the S/N of low-γ nuclei, where the polarization transfer efficiency largely relies on the dipolar couplings between proton and low-γ nuclei. As a result, polarization transfer can be difficult if heteronuclear dipolar couplings are greatly averaged out by molecular motions, as often encountered for the mobile components in semi-solids or multiphase heterogeneous systems. To enhance the S/N of mobile components, we recently demonstrated a method for acquiring 1D ^{13}C MAS spectrum by combining CP with transient heteronuclear nuclear Overhauser effect (NOE) and refocused insensitive nuclei enhanced by polarization transfer (RINEPT), dubbed as CP-NOE and CP-RINEPT, respectively [56]. For a multi-component system, the ^{13}C signals from rigid components are enhanced by CP, while the signals from mobile components are enhanced by either heteronuclear NOE or RINEPT. In addition, the CP-RINEPT experiment enables the acquisition of two separate spectra, each of which contains signals from either rigid or mobile components alone.

In this study, we propose two 2D HETCOR pulse sequences further utilizing NOE or RINEPT to enhance the ^{13}C signals of mobile components. The ^{13}C-detected HETCOR experiment can be used under slow MAS speeds, where a multiple-pulse sequence is employed to enhance the ^{1}H resolution in the indirect dimension. On the other hand, the ^{1}H-detected HETCOR experiment should be performed under very fast MAS, where the sensitivity is enhanced by the combination of CP and heteronuclear NOE via ^{1}H detection. Compared to the regular 2D HETCOR experiment, the proposed method offers the acquisition of two separate 2D HETCOR spectra for rigid alone and mobile alone components of a multiphase system with barely increasing the overall experimental time. Herein, the 2D HETCOR spectra obtained for rigid and mobile components are denoted as Rigid-HETCOR and Mobile-HETCOR, respectively. The benefits and possible limitations of the two proposed methods are discussed within the context of their applications to study polymer blend systems.

2. Radio-frequency pulse schemes

The radio-frequency (RF) pulse sequences demonstrated in this study are shown in Fig. 1. The ^{13}C-detected 2D HETCOR NMR experiment (Fig. 1a) is designed for a moderate MAS frequency. In this sequence, during the t_1 period, the transverse ^{1}H magnetization is allowed to evolve under frequency-switched or phase-modulated Lee-Goldburg (FSLG) [57–60] pulse sequence that is used to suppress ^{1}H-^{1}H dipolar couplings. While the transverse ^{1}H magnetization from rigid components is transferred to ^{13}C using CP, those from the mobile components are kept spin-locked during CP. During the first signal acquisition period for the Rigid-HETCOR spectrum, high power continuous-wave (CW) RF decoupling is applied to achieve high spectral resolution and also to retain the transverse ^{1}H magnetization by spin-locking for the subsequent RINEPT-based magnetization transfer. While the RINEPT sequence transfers the transverse ^{1}H magnetization from mobile components, it also suppresses the ^{1}H magnetization from rigid components due to their short T_2 relaxation, and thus enables recording Mobile-HETCOR spectrum through the second t_2 acquisition period.

A ^{1}H-detected HETCOR NMR pulse sequence for experiments under fast-MAS is shown in Fig. 1b. After the initial CP period, the transverse ^{13}C magnetization is flipped to the +z direction for storage, and HORROR pulse sequence [61] is applied to remove any residual ^{1}H magnetization before $^{13}C \rightarrow {}^{1}H$ CP. Notably, the HORROR sequence not only removes the residual proton magnetization before signal detection, but also enhances the ^{13}C signals from mobile components by using the steady-state heteronuclear NOE effect as shown in Fig. S1. Interestingly, the signal intensity of the methyl group of the rigid PMMA components can even be enhanced by the use of HORROR sequence as shown in Fig. S2. The ^{13}C magnetization from the rigid components is transferred to ^{1}H by the second CP for the first signal acquisition during t_2 (to obtain the 2D Rigid-HETCOR spectrum). On the other hand, the ^{13}C magnetization from the mobile components is spin-locked during the $^{13}C \rightarrow {}^{1}H$ CP contact time and subsequent CW decoupling periods, and then transferred to protons by RINEPT

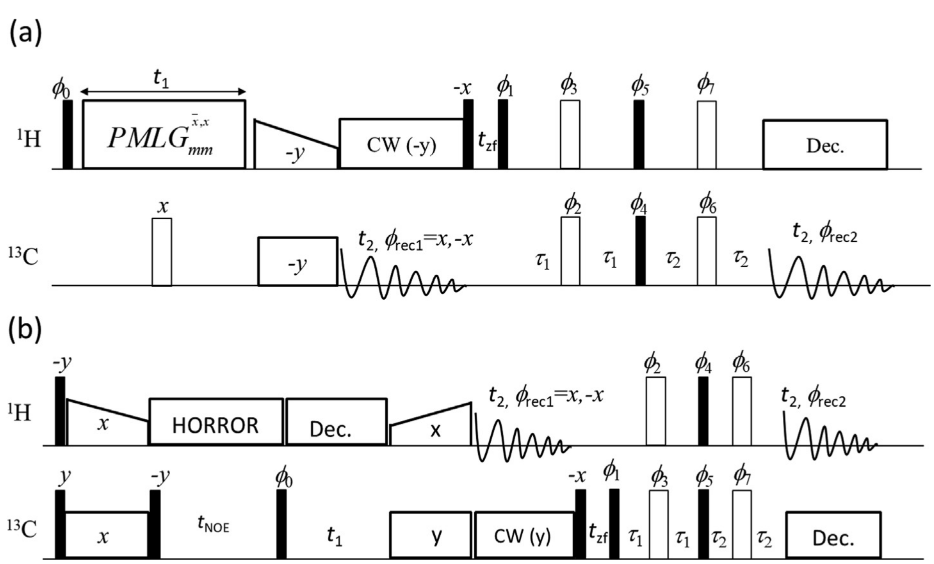

Fig. 1. 2D ^{13}C-detected (a) and ^{1}H-detected (b) 2D HETCOR NMR pulse sequences applied under slow and very fast MAS, respectively. The black solid and blank rectangles indicate 90° and 180° pulses, respectively. Phase cycling schemes used in the HETCOR experiments are: $\phi_0 = x,-x$; $\phi_1 = 16(x),16(-x)$; $\phi_2 = \phi_3 = 2(x),2(-x)$; $\phi_4 = 8(x), 8(y), 8(-x), 8(-y)$; $\phi_5 = 4(y), 4(-y)$; $\phi_6 = 2(x), 2(-x), 2(x), 2(-x), 2(y), 2(-y), 2(y), 2(-y)$; $\phi_7 = 2(x), 2(-x)$; $\phi_{rec2} = 2(x, -x), 2(-x, x), 2 (y, -y), 2(-y, y)$.

for the second signal acquisition during t_2 (Mobile-HETCOR). During signal acquisitions of rigid and mobile components, $^{13}C \rightarrow {}^{1}H$ dipolar coupling can be decoupled as indicated in the pulse sequence. It may be noted that using the pulse sequence shown in Fig. 1b, there is about 10–20% signal loss for the mobile components (PB) as compared to the standard RINEPT-based HETCOR experiment (Fig. S1). However, the total experimental time for acquiring the Rigid- and Mobile-HETCOR spectra is nearly the same as that for the standard double-CP based HETCOR experiment since there is only a few tens of milliseconds additional time required for each scan. In other words, RINEPT-based HETCOR spectrum can be obtained by the cost of 10–20% signal loss with negligible experimental time.

3. Experimental details

3.1. Materials

The hydroxyl-terminated 1,4-polybutadiene (PB, Fig. 2) oligomers were purchased from Xiensi Reagent Company (Tianjin, China). All the other samples were purchased from Aldrich Co., and used as received without any further purification. Molecular weights of poly(methyl methacrylate) (PMMA, Fig. 2) and PB are 100,000 g/mol and 5000 g/mol, respectively. The glycine/adamantane mixture was prepared with a 1:1 weight ratio. The PMMA/PB blend was prepared by mechanically mixing PMMA and PB in a 4:1 weight ratio.

3.2. Solid-State NMR experiments

The ^{13}C-detected HETCOR NMR experiment (Fig. 1a) for PMMA/PB blend was performed on a Varian 400 MHz VNMRS solid-state NMR spectrometer equipped with a 5 mm triple-resonance MAS probe. The spinning speed was actively controlled at 8 kHz with a MAS speed controller. The ^{1}H and ^{13}C resonance frequencies were 400.11 MHz and 100.62 MHz, respectively. The 90° pulse widths were 3.2 μs for ^{1}H and 4.4 μs for ^{13}C, respectively. The effective FSLG decoupling field strength was 95.7 kHz, corresponding to a frequency offset of 55.3 kHz. Ramped-CP with a 5% ramp on the ^{1}H channel was used to transfer ^{1}H magnetization to ^{13}C. The RINEPT evolution times, τ_1 and τ_2, were set to 1.4 ms and 1.0 ms, respectively. The CP contact time was set as 100 μs in order to obtain only the bonded ^{13}C-^{1}H chemical shift correlation in the final 2D HETCOR spectra. The acquisition time was about 10 ms for each of the signal acquisition periods. The ^{13}C-detected HETCOR NMR experiment (Fig. 1a) for glycine/adamantane mixture was performed on a 600 MHz ECZ600R solid-state NMR spectrometer equipped with a 2.0 mm double-resonance MAS probe (JEOL Resonance Inc) under a spinning speed of 8 kHz. The 90° pulse widths were 1.6 μs and 2 μs for ^{1}H and ^{13}C nuclei, respectively. The CP contact time was 0.2 ms and both RINEPT evolution times, τ_1 and τ_2, were set to 0.5 ms. The recycle delay was 10 s, and the acquisition time was around 6.8 ms.

The ^{1}H-detected HETCOR experiment was performed under 70 kHz MAS on a 600 MHz ECZ600R solid-state NMR spectrometer equipped with a 1.0 mm double-resonance ultrafast MAS probe (JEOL Resonance Inc). The 90° pulse widths were 0.8 and 1.15 μs

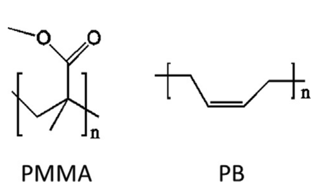

Fig. 2. Chemical structures of PMMA and PB used in this study.

for ^{1}H and ^{13}C nuclei, respectively. Both the RINEPT evolution times, τ_1 and τ_2, were set to 1.5 ms. The recycle delay was 6.5 s and 1.5 s for the experiment on glycine/adamantane mixture and PMMA/PB blend, respectively. The acquisition time was set about 8.2 ms for both first and second acquisition periods. For the experiment on glycine/adamantane, the t_1 evolution time was around 8.5 ms, while it was around 6.8 ms for PMMA/PB blend. Using the same RF field strength for ^{1}H decoupling and HORROR sequence can avoid the buildup of proton magnetization during the t_1 evolution period, and thus reduce the t_1 noise.

For both ^{13}C and ^{1}H-detected HETCOR experiments shown in Fig. 1a and b, a z-filter was inserted right after the first signal acquisition period to remove the residual magnetization in the transverse plane. The ^{13}C and ^{1}H chemical shifts were referenced with respect to TMS using the low-frequency ^{13}C peak (δ_{iso} = 29.4 ppm) and ^{1}H peak (δ_{iso} = 1.9 ppm) of adamantane. Two 2D HETCOR spectra can be obtained from a single experiment, which are denoted as Rigid-HETCOR and Mobile-HETCOR spectra.

4. Results and discussion

Molecular motion plays a critical role in most molecular systems, which may significantly affect the physical, chemical and functional properties of a material [62–64]. For example, the mobile components in a multiphase polymer system can significantly increase the toughness of the material, and thus lead to an enhancement of stretching extensibility. Although such polymeric materials are not amenable for atomic-resolution studies for most analytical techniques, they can be investigated at atomic-resolution using a variety of solid-state NMR techniques that have no limitation on the molecular size and nature of the material. However, in a typical CP based MAS experiment, the signals of mobile components are greatly compromised or even lost due to the their weak ^{1}H-^{13}C heteronuclear dipolar couplings, rendering the traditional CP-based HETCOR experiment incapable to detect ^{1}H/^{13}C chemical shift correlations of mobile components. In order to address this issue, herein we have successfully demonstrated two HETCOR pulse sequences (Fig. 1) suitable for measurements under slow and very fast MAS conditions, enabling the acquisition of 2D HETCOR NMR spectra of rigid and mobile components in a single experiment with barely increasing the overall experimental time by making use of a single recycle delay. To demonstrate the efficacy of the proposed pulse sequences, a glycine and adamantane mixture was first used as a model system before applying the techniques on a complex polymer blend. Glycine is a rigid crystalline small molecule with α or γ form stable crystallites, while adamantane can be considered as a mobile component since its fast molecular rotations significantly suppress intramolecular ^{1}H-^{1}H dipolar interactions. It should be noted that residual ^{1}H-^{1}H and ^{1}H-^{13}C intermolecular interactions remain in adamantane since it is a plastic crystal. Indeed, the Rigid-HETCOR spectrum shown in Fig. 3a obtained using the ^{13}C-detected HETCOR pulse sequence (Fig. 1a) gives both glycine and adamantane signals even with a very short contact time of 0.2 ms. This is because the presence of ^{1}H-^{1}H homonuclear dipolar interactions speeds up the ^{1}H-->^{13}C CP build-up in addition to residual intermolecular ^{13}C-^{1}H dipolar couplings in adamantane. However, in the Mobile-HETCOR spectra shown in Fig. 3b, only adamantane signals were observed due to the use of RINEPT sequence, where the rigid glycine signals are suppressed by the fast spin-spin relaxation during the evolution periods (τ_1 and τ_2). These spectra also demonstrate the use of PMLG in the t_1 (i.e. ^{1}H) dimension to obtain narrow proton peaks under a slow spinning speed.

Using the pulse sequence shown in Fig. 1b, 1H-detected 2D HETCOR spectrum obtained from glycine/adamantane mixture

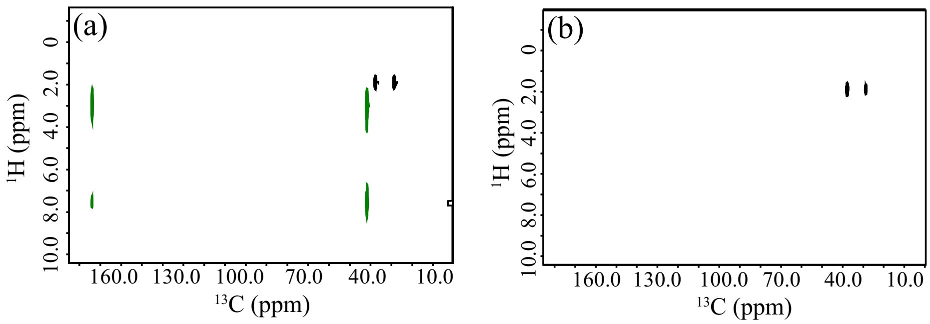

Fig. 3. ^{13}C-detected HETCOR spectra of a glycine/adamantane mixture under 8 kHz MAS: Rigid-HETCOR (a) and Mobile-HETCOR (b) spectra were obtained from a single experiment using the pulse sequence shown in Fig. 1a. The CP contact time was 0.2 ms, and both RINEPT evolution times, τ_1 and τ_2, were 0.5 ms. The signals of adamantane were indicated in black, while that from glycine are in green. (For interpretation of the references to colour in this figure legend, the reader is referred to the web version of this article.)

under 70 kHz MAS is shown in Fig. 4. For a direct comparison, the Rigid-HETCOR and Mobile-HETCOR spectra are superimposed. We did not observe any adamantane signal in the Rigid-HETCOR spectrum at 70 kHz MAS, although the second CP contact time of 0.4 ms is longer than that used for experiments at 8 kHz MAS. This is because the CP build-up curve is dominated by the weak intermolecular heteronuclear dipolar interactions due to the suppression of ^{1}H-^{1}H dipolar interactions under 70 kHz MAS. Because of this, signals from glycine and adamantane are well separated, and two independent HETCOR spectra corresponding to that of glycine and adamantane are obtained in a single experiment. It should be noted that we did not observe any separation in CH_2 proton peaks for glycine in the Rigid-HETCOR spectrum, since the glycine crystallite is in the γ form. The capabilities of ultrafast MAS as well as the multiple-pulse sequence in resolving the two proton peaks of α form glycine crystallites have been well demonstrated in multiple studies [65,66]. In this study, we have demonstrated the performance of ^{13}C-detected and ^{1}H-detected HETCOR pulse sequences to obtain 2D ^{13}C/^{1}H HETCOR spectra of rigid and mobile components separately in a single experiment.

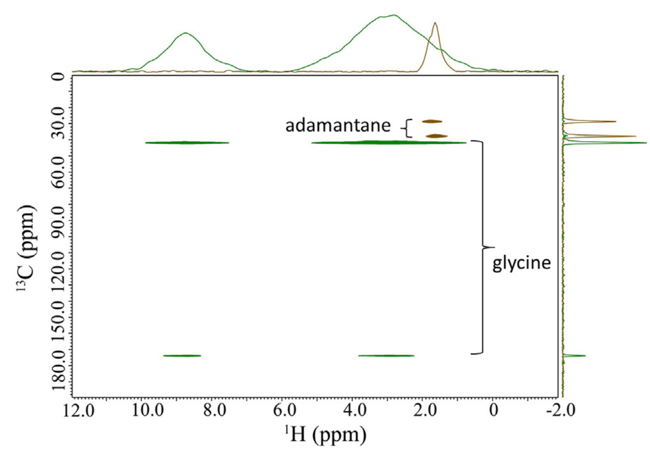

Fig. 4. ^{1}H-detected HETCOR spectra of glycine/adamantane mixture under 70 kHz MAS. The superimposed Rigid-HETCOR (green) and Mobile-HETCOR (brown) spectra were obtained from a single experiment using the pulse sequence shown in Fig. 1b. 1 and 0.4 ms for the first and second CP contact times, respectively, were used. HORROR sequence for 0.5 s was used to remove the residual proton magnetization before detection and also to enable the NOE-based polarization transfer for enhancing signals from mobile components. (For interpretation of the references to colour in this figure legend, the reader is referred to the web version of this article.)

Polymer blend has many technological applications and is widely used in industry since the merits of two different bulk materials can be combined and the end-use properties (*eg.* mechanical and rheological) can be optimized [67–70]. In this study, we further demonstrated the robust performance of the proposed pulse sequences on polymer blend PMMA/PB; their chemical structures are shown in Fig. 2. PMMA is a semi-crystalline polymer with glass transition (T_g) and melting (T_m) temperatures both above 100 °C, whereas PB is a viscous liquid with a T_g of ~−90 °C. Therefore, in the PMMA/PB blend, PMMA is considered as the rigid and PB is the mobile components at room temperature. It was previously shown that in such a polymer blend system with a significant mobility contrast for the components, the ^{13}C signals of PB cannot be detected by CP [56], because the ^{13}C-^{1}H dipolar couplings have been completely averaged out by the fast molecular motion of PB. However, the ^{13}C signals of such mobile components can be detected by the RINEPT sequence or transient heteronuclear NOE [56]. Herein, using a combination of CP and RINEPT and/or NOE, ^{13}C-detected and ^{1}H-detected HETCOR (Fig. 1) experiments can be used to obtain the ^{13}C/^{1}H HETCOR spectra of such polymer blend, where the HETCOR spectra of rigid and mobile components can be separately obtained in a single experiment with barely increasing the experimental time as compared to the standard HETCOR experiment. The 2D HETCOR spectra of the PMMA/PB blend are shown in Figs. 5 and 6. The Rigid-HETCOR spectrum exhibits signals only from rigid PMMA, while Mobile-HETCOR spectrum displays the mobile PB signals. It may be noted that the proton peaks of PB signals in Mobile-HETCOR spectrum appears to be very broad, which can be attributed to the presence of different conformation (trans- and cis- 1,4-units, ~80%), the vinyl-1,2-units and end-groups in PB chains [71]; and also partly due to truncation of signal as the t_1 evolution time may be insufficient and the use of an exponential line broadening factor of 100 Hz in t_1 during 2D Fourier transformation to reduce the noise. However, the trans- and cis- 1,4-units in PB still dominate the signals, and thus clear ^{13}C/^{1}H chemical shift correlations can be observed for the dominating cis- and trans- 1,4-PB chains. Note that the low intensity peaks in Fig. 5b observed at ~143 ppm, 115 ppm, 45 ppm, 39 ppm, and 31 ppm are ascribed to the minute vinyl-1,2-units and end-group units; these peaks are also be observed in Fig. 6b despite of their low abundance in PMMA/PB blend, which further demonstrate the high sensitivity and robust performance of the proposed pulse sequences to sequentially acquire Rigid-HETCOR and Mobile-HETCOR spectra in a single experiment. In addition, in the ^{1}H-detected 2D Mobile-HETCOR spectra (Fig. 6b), the direct detection of proton signals after the RINEPT sequence also results in higher signal intensity when compared to the ^{13}C-detected case, since a much longer acquisition time and shorter dwell time can be used along with/without low-power RF decoupling on the ^{13}C channel. For the two pulse sequences, the continuous-wave (CW) decoupling has to be

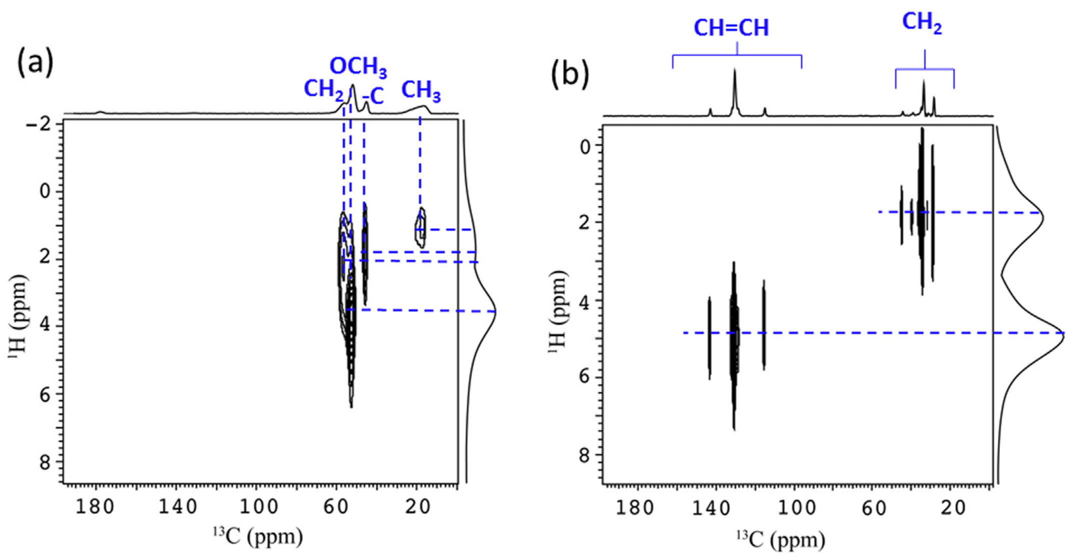

Fig. 5. ^{13}C-detected HETCOR spectra of PMMA/PB blend obtained under 8 kHz MAS: Rigid-HETCOR (a) and Mobile-HETCOR (b) spectra were obtained from a single experiment using the pulse sequence shown in Fig. 1a. 0.1 ms CP contact time and the RINEPT evolution times, τ_1 and τ_2, of 1.4 ms and 1.0 ms, respectively, were used. FSLG was used here for obtaining narrow proton peaks.

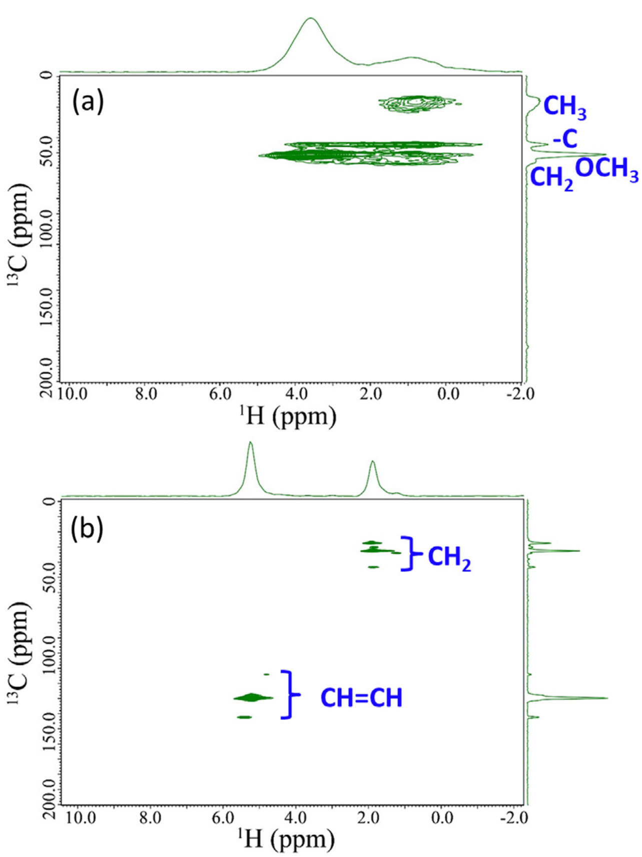

Fig. 6. ^{1}H-detected HETCOR spectra of PMMA/PB blend obtained under 70 kHz MAS: Rigid-HETCOR (a) and Mobile-HETCOR (b) spectra were obtained simultaneously from a single experiment using the pulse sequence shown in Fig. 1b. First and second CP contact times were 1 and 0.4 ms, respectively. HORROR sequence for 0.5 s was used to remove the residual proton magnetization before detection and also to enable the NOE-based polarization transfer for enhancing signals from mobile components.

applied during the signal acquisition after CP in order to keep the transverse magnetization of mobile components for the subsequent polarization transfer by RINEPT. For the ^{13}C-detected HETCOR experiment (Fig. 1a), CW decoupling might potentially compromise ^{13}C spectral resolution of rigid components. However, it should be noted that in the multiphase solids, the mobility of rigid components is generally enhanced by the mobile components; thus CW decoupling with high RF strength can still provide a good spectral resolution as demonstrated in our previous study [56]. Notably, both the ^{13}C- and ^{1}H-detected HETCOR experimental time is nearly the same as that of the traditional ^{13}C- and ^{1}H-detected CP-based HETCOR experiment, respectively, because only a few milliseconds additional time for each scan is required to complete the experiment.

Indeed, in terms of shortening experimental time as well as enhancing signal sensitivity of multi-dimensional solid-state NMR experiments, several approaches and strategies have been proposed to enable multiple acquisition in a single scan, either through elegant designs of pulse sequences or with the use of multiple receivers [72–77]. In those multi-acquisition experiments, the ^{13}C or ^{15}N magnetizations are generally re-utilized as the source for polarization transfer after the first acquisition period, because the ^{13}C or ^{15}N magnetization is easy to store due to the very long spin-lattice relaxation time (T_1) of these nuclei. However, the use of residual proton magnetization is much more challenging due to its generally short T_1 and $T_{1\rho}$ in typical solids, but greatly beneficial for the signal enhancement of low-γ nuclei as demonstrated by our work here and previous studies [56,78]. Fortunately, in the multiphase solids, the mobile components generally exhibit a very long T_2 and $T_{1\rho}$; therefore, the proton magnetization of mobile components can be further utilized to enhance the signal intensity and to obtain 2D HETCOR spectra of mobile components.

5. Conclusions

In multi-component solids with mobility contrast, the ^{13}C signals of mobile components are undetectable in the regular CP-based HETCOR experiment due to insufficiency of CP for polarization transfer, since the ^{1}H-^{13}C dipolar couplings are averaged out by the fast molecular motions. Herein, we have proposed two novel HETCOR pulse sequences (^{13}C- and ^{1}H-detected HETCOR) suitable for measurement under slow and ultrafast MAS conditions by fully utilizing the abundant proton magnetization for polarization transfer. From a single experiment, two HETCOR spectra, through the polarization transfer based on CP and RINEPT, can be obtained corresponding to that of rigid and mobile components, respectively. In the ^{1}H-detected HETCOR experiment, heteronuclear NOE was well combined with CP to significantly enhance the ^{13}C magnetization of mobile components in the indirect dimension, and thus enables the subsequent $^{13}C \rightarrow {}^1H$ polarization transfer with RINEPT sequence. While two HETCOR spectra can be obtained from such a single experiment, the experimental time barely increases, as compared to the single conventional CP and RINEPT-based HETCOR experiment. Thus, the total experimental time was significantly reduced when compared to the total time needed to measure two conventional CP and RINEPT-based HETCOR experiment to obtain HETCOR spectra for rigid and mobile components, respectively. In addition to the significant reduction of data collection time, the separation of signals from mobile and rigid components can also be potentially used for resonance assignment in a wide array of multiphase heterogeneous systems. Thus, we believe the proposed sequences here will greatly beneficial for the structural elucidation of complex systems, such as biomaterials, polymer blends, proteins, supramolecular assemblies and so on. For example, atomic-resolution investigation of the ubiquitous self-assembly process underlying the formation of nanostructures including amyloid fibrils, using the proposed 2D HETCOR pulse sequences, would enable selective monitoring of fast-tumbling monomers and small oligomers even in the presence of large aggregates or fibers [79]. Such experiments can shed light on the nucleation of small oligomeric amyloid intermediates that have been shown to be more toxic in the amyloid diseases like Alzheimer's Disease and type II diabetes. Such approaches can also be potentially used to probe weak drug-polymer interactions in pharmaceutical compounds [80] and to observe the fast dynamics of lipids in membrane bilayers [81].

Acknowledgments

We acknowledge the funding support from the National Institutes of Health (GM084018 to A.R.). This work was supported by JSPS KAKENHI Grant (JP17H03043 to Y.N.).

Appendix A. Supplementary material

Supplementary data to this article can be found online at https://doi.org/10.1016/j.jmr.2019.106615.

References

[1] T. Schubeis, T. Le Marchand, L.B. Andreas, G. Pintacuda, 1H magic-angle spinning NMR evolves as a powerful new tool for membrane proteins, J. Magn. Reson. 287 (2018) 140–152.
[2] M. Tang, G. Comellas, C.M. Rienstra, Advanced solid-state NMR approaches for structure determination of membrane proteins and amyloid fibrils, Acc. Chem. Res. 46 (2013) 2080–2088.
[3] L.A. Baker, M. Baldus, Characterization of membrane protein function by solid-state NMR spectroscopy, Curr. Opin. Struct. Biol. 27 (2014) 48–55.
[4] S. Wang, V. Ladizhansky, Recent advances in magic angle spinning solid state NMR of membrane proteins, Prog. Nucl. Magn. Reson. Spectrosc. 82 (2014) 1–26.
[5] V.S. Mandala, J.K. Williams, M. Hong, Structure and dynamics of membrane proteins from solid-state NMR, Annu. Rev. Biophys. 47 (2018) 201–222.
[6] H.W. Spiess, 50th Anniversary perspective: the importance of NMR spectroscopy to macromolecular Science, Macromolecules 50 (2017) 1761–1777.
[7] M.R. Hansen, R. Graf, H.W. Spiess, Interplay of structure and dynamics in functional macromolecular and supramolecular systems as revealed by magnetic resonance spectroscopy, Chem. Rev. 116 (2015) 1272–1308.
[8] K. Schmidt-Rohr, H.W. Spiess, Multidimensional Solid-State NMR and Polymers, Academic Press, London, 1994.
[9] R. Zhang, T. Miyoshi, P. Sun (Eds.), NMR Methods for Characterization of Synthetic and Natural Polymers, Royal Society of Chemistry Publishing, 2019.
[10] K.H. Mroue, A. Viswan, N. Sinha, A. Ramamoorthy, Solid-state NMR spectroscopy: the magic wand to view bone at nanoscopic resolution, Annu. Rep. NMR Spectrosc. 92 (2017) 365–413.
[11] M.J. Duer, The contribution of solid-state NMR spectroscopy to understanding biomineralization: atomic and molecular structure of bone, J. Magn. Reson. 253 (2015) 98–110.
[12] Y.-Y. Hu, A. Rawal, K. Schmidt-Rohr, Strongly bound citrate stabilizes the apatite nanocrystals in bone, Proc. Natl. Acad. Sci. USA 107 (2010) 22425–22429.
[13] T. Theint, P.S. Nadaud, D. Aucoin, J.J. Helmus, S.P. Pondaven, K. Surewicz, W.K. Surewicz, C.P. Jaroniec, Species-dependent structural polymorphism of Y145Stop prion protein amyloid revealed by solid-state NMR spectroscopy, Nat. Comm. 8 (2017) 753.
[14] M. Lee, T. Wang, O.V. Makhlynets, Y. Wu, N.F. Polizzi, H. Wu, P.M. Gosavi, J. Stöhr, I.V. Korendovych, W.F. DeGrado, Zinc-binding structure of a catalytic amyloid from solid-state NMR, Proc. Natl. Acad. Sci. USA 114 (2017) 6191–6196.
[15] Z. Niu, W. Zhao, Z. Zhang, F. Xiao, X. Tang, J. Yang, The molecular structure of Alzheimer β-amyloid fibrils formed in the presence of phospholipid vesicles, Angew. Chem. Int. Ed. 53 (2014) 9294–9297.
[16] W. Qiang, W.-M. Yau, J.-X. Lu, J. Collinge, R. Tycko, Structural variation in amyloid-β fibrils from Alzheimer's disease clinical subtypes, Nature 541 (2017) 217.
[17] L. Lecoq, T. Wiegand, F.J. Rodriguez-Alvarez, R. Cadalbert, G.A. Herrera, L. del Pozo-Yauner, B.H. Meier, A. Böckmann, A substantial structural conversion of the native monomer leads to in-register parallel amyloid fibril formation in light-chain amyloidosis, Chembiochem 20 (2019) 1027–1031.
[18] A. Mainz, J. Peschek, M. Stavropoulou, K.C. Back, B. Bardiaux, S. Asami, E. Prade, C. Peters, S. Weinkauf, J. Buchner, B. Reif, The chaperone αB-crystallin uses different interfaces to capture an amorphous and an amyloid client, Nat. Struct. Mol. Biol. 22 (2015) 898.
[19] Y. Gao, R. Zhang, W. Lv, Q. Liu, X. Wang, P. Sun, H.H. Winter, G. Xue, Critical effect of segmental dynamics in polybutadiene/clay nanocomposites characterized by solid state 1H NMR spectroscopy, J. Phys. Chem. C 118 (2014) 5606–5614.
[20] J. Brus, M. Urbanová, I. Kelnar, J. Kotek, A Solid-state NMR study of structure and segmental dynamics of semicrystalline elastomer-toughened nanocomposites, Macromolecules 39 (2006) 5400–5409.
[21] C. Bonhomme, C. Gervais, D. Laurencin, Recent NMR developments applied to organic-inorganic materials, Prog. Nucl. Magn. Reson. Spectrosc. 77 (2014) 1–48.
[22] Q. Dang, S. Lu, S. Yu, P. Sun, Z. Yuan, Silk fibroin/montmorillonite nanocomposites: effect of pH on the conformational transition and clay dispersion, Biomacromolecules 11 (2010) 1796–1801.
[23] K. Takegoshi, S. Nakamura, T. Terao, 13C–1H dipolar-assisted rotational resonance in magic-angle spinning NMR, Chem. Phys. Lett. 344 (2001) 631–637.
[24] M. Shen, B. Hu, O. Lafon, J. Trébosc, Q. Chen, J.-P. Amoureux, Broadband finite-pulse radio-frequency-driven recoupling (fp-RFDR) with (XY8)41 super-cycling for homo-nuclear correlations in very high magnetic fields at fast and ultra-fast MAS frequencies, J. Magn. Reson. 223 (2012) 107–119.
[25] J.R. Lewandowski, G.D. Paepe, M.T. Eddy, R.G. Griffin, 15N–15N proton assisted recoupling in magic angle spinning NMR, J. Am. Chem. Soc. 131 (2009) 5769–5776.
[26] Y. Ishii, 13C–13C dipolar recoupling under very fast magic angle spinning in solid-state nuclear magnetic resonance: applications to distance measurements, spectral assignments, and high-throughput secondary-structure determination, J. Chem. Phys. 114 (2001) 8473–8483.
[27] Y. Jayasubba Reddy, V. Agarwal, A. Lesage, L. Emsley, K.V. Ramanathan, Heteronuclear proton double quantum-carbon single quantum scalar correlation in solids, J. Magn. Reson. 245 (2014) 31–37.
[28] D.H. Zhou, G. Shah, M. Cormos, C. Mullen, D. Sandoz, C.M. Rienstra, Proton-detected solid-state NMR spectroscopy of fully protonated proteins at 40 kHz magic-angle spinning, J. Am. Chem. Soc. 129 (2007) 11791–11801.
[29] G.P. Holland, Q. Mou, J.L. Yarger, Determining hydrogen-bond interactions in spider silk with 1H–13C HETCOR fast MAS solid-state NMR and DFT proton chemical shift calculations, Chem. Commun. 49 (2013) 6680–6682.
[30] B.-J. Van Rossum, C. De Groot, V. Ladizhansky, S. Vega, H. De Groot, A method for measuring heteronuclear (1H–13C) distances in high speed MAS NMR, J. Am. Chem. Soc. 122 (2000) 3465–3472.
[31] S.M. Althaus, K. Mao, J.A. Stringer, T. Kobayashi, M. Pruski, Indirectly detected heteronuclear correlation solid-state NMR spectroscopy of naturally abundant 15N nuclei, Solid State Nucl. Magn. Reson. 57–58 (2014) 17–21.
[32] K. Mao, M. Pruski, Directly and indirectly detected through-bond heteronuclear correlation solid-state NMR spectroscopy under fast MAS, J. Magn. Reson. 201 (2009) 165–174.
[33] M.D. Tuttle, G. Comellas, A.J. Nieuwkoop, D.J. Covell, D.A. Berthold, K.D. Kloepper, J.M. Courtney, J.K. Kim, A.M. Barclay, A. Kendall, Solid-state NMR structure of a pathogenic fibril of full-length human α-synuclein, Nat. Struct. Mol. Biol. 23 (2016) 409.
[34] V. Agarwal, S. Penzel, K. Szekely, R. Cadalbert, E. Testori, A. Oss, J. Past, A. Samoson, M. Ernst, A. Böckmann, De Novo 3D structure determination from sub-milligram protein samples by solid-state 100 kHz MAS NMR spectroscopy, Angew. Chem. Int. Ed. 53 (2014) 12253–12256.
[35] A. Marchanka, B. Simon, G. Althoff-Ospelt, T. Carlomagno, RNA structure determination by solid-state NMR spectroscopy, Nat. Commun. 6 (2015) 7024.
[36] J.-P. Demers, B. Habenstein, A. Loquet, S.K. Vasa, K. Giller, S. Becker, D. Baker, A. Lange, N.G. Sgourakis, High-resolution structure of the Shigella type-III secretion needle by solid-state NMR and cryo-electron microscopy, Nat. Commun. 5 (2014) 4976.

[37] S. Wang, R.A. Munro, L. Shi, I. Kawamura, T. Okitsu, A. Wada, S.-Y. Kim, K.-H. Jung, L.S. Brown, V. Ladizhansky, Solid-state NMR spectroscopy structure determination of a lipid-embedded heptahelical membrane protein, Nat. Meth. 10 (2013) 1007–1012.
[38] S. Yan, C.L. Suiter, G. Hou, H. Zhang, T. Polenova, Probing structure and dynamics of protein assemblies by magic angle spinning NMR spectroscopy, Acc. Chem. Res. 46 (2013) 2047–2058.
[39] G. Hou, S. Yan, S. Sun, Y. Han, I.-J.L. Byeon, J. Ahn, J. Concel, A. Samoson, A.M. Gronenborn, T. Polenova, Spin diffusion driven by R-symmetry sequences: applications to homonuclear correlation spectroscopy in MAS NMR of biological and organic solids, J. Am. Chem. Soc. 133 (2011) 3943–3953.
[40] V. Kurauskas, E. Crublet, P. Macek, R. Kerfah, D.F. Gauto, J. Boisbouvier, P. Schanda, Sensitive proton-detected solid-state NMR spectroscopy of large proteins with selective CH3 labelling: application to the 50S ribosome subunit, Chem. Commun. 52 (2016) 9558–9561.
[41] R. Zhang, K.H. Mroue, A. Ramamoorthy, Proton-based ultrafast magic angle spinning solid-state NMR spectroscopy, Acc. Chem. Res. 50 (2017) 1105–1113.
[42] Y. Nishiyama, Fast magic-angle sample spinning solid-state NMR at 60–100 kHz for natural abundance samples, Solid State Nucl. Magn. Reson. 78 (2016) 24–36.
[43] R. Zhang, Y. Nishiyama, P. Sun, A. Ramamoorthy, Phase cycling schemes for finite-pulse-RFDR MAS solid state NMR experiments, J. Magn. Reson. 252 (2015) 55–66.
[44] A. Krajnc, T. Kos, N. Zabukovec Logar, G. Mali, A simple NMR-based method for studying the spatial distribution of linkers within mixed-linker metal-organic frameworks, Angew. Chem. Int. Ed. 54 (2015) 10535–10538.
[45] A.J. Rossini, M.P. Hanrahan, M.M. Thuo, Rapid acquisition of Wideline MAS solid-state NMR spectra with fast MAS, indirect proton detection, and dipolar HMQC pulse sequences, Phys. Chem. Chem. Phys. 18 (2016) 25284–25295.
[46] P. Fricke, V. Chevelkov, M. Zinke, K. Giller, S. Becker, A. Lange, Backbone assignment of perdeuterated proteins by solid-state NMR using proton detection and ultrafast magic-angle spinning, Nat. Protoc. 12 (2017) 764.
[47] D. Mukhopadhyay, P.S. Nadaud, M.D. Shannon, C.P. Jaroniec, Rapid quantitative measurements of paramagnetic relaxation enhancements in Cu (II)-tagged proteins by proton-detected solid-state NMR spectroscopy, J. Phys. Chem. Lett. 8 (2017) 5871–5877.
[48] J. Tolchard, M.K. Pandey, M. Berbon, A. Noubhani, S.J. Saupe, Y. Nishiyama, B. Habenstein, A. Loquet, Detection of side-chain proton resonances of fully protonated biosolids in nano-litre volumes by magic angle spinning solid-state NMR, J. Biomol. NMR 70 (2018) 177–185.
[49] L.B. Andreas, T. Le Marchand, K. Jaudzems, G. Pintacuda, High-resolution proton-detected NMR of proteins at very fast MAS, J. Magn. Reson. 253 (2015) 36–49.
[50] Y. Ishii, J.P. Yesinowski, R. Tycko, Sensitivity enhancement in solid-state 13C NMR of synthetic polymers and biopolymers by 1H NMR detection with high-speed magic angle spinning, J. Am. Chem. Soc. 123 (2001) 2921–2922.
[51] R. Bernd, Ultra-high resolution in MAS solid-state NMR of perdeuterated proteins: Implications for structure and dynamics, J. Magn. Reson. 216 (2012) 1–12.
[52] S.K. Vasa, P. Rovó, R. Linser, Protons as versatile reporters in solid-state NMR spectroscopy, Acc. Chem. Res. 51 (2018) 1386–1395.
[53] E.K. Paulson, C.R. Morcombe, V. Gaponenko, B. Dancheck, R.A. Byrd, K.W. Zilm, Sensitive high resolution inverse detection NMR spectroscopy of proteins in the solid state, J. Am. Chem. Soc. 125 (2003) 15831–15836.
[54] J. Schaefer, E. Stejskal, Carbon-13 nuclear magnetic resonance of polymers spinning at the magic angle, J. Am. Chem. Soc. 98 (1976) 1031–1032.
[55] A. Pines, M. Gibby, J. Waugh, Proton-enhanced NMR of dilute spins in solids, J. Chem. Phys. 59 (1973) 569–590.
[56] R. Zhang, K.H. Mroue, A. Ramamoorthy, Hybridizing cross-polarization with NOE or refocused-INEPT enhances the sensitivity of MAS NMR spectroscopy, J. Magn. Reson. 266 (2016) 59–66.
[57] A. Bielecki, A. Kolbert, M. Levitt, Frequency-switched pulse sequences: homonuclear decoupling and dilute spin NMR in solids, Chem. Phys. Lett. 155 (1989) 341–346.
[58] M. Leskes, P.K. Madhu, S. Vega, A broad-banded z-rotation windowed phase-modulated Lee-Goldburg pulse sequence for 1H spectroscopy in solid-state NMR, Chem. Phys. Lett. 47 (2007) 370–374.
[59] M. Lee, W.I. Goldburg, Nuclear-magnetic-resonance line narrowing by a rotating rf field, Phys. Rev. 140 (1965) A1261.
[60] M. Mehring, J. Waugh, Magic-angle NMR experiments in solids, Phys. Rev. B 5 (1972) 3459.
[61] N.C. Nielsen, H. Bildso/e, H.J. Jakobsen, M.H. Levitt, Double-quantum homonuclear rotary resonance: efficient dipolar recovery in magic-angle spinning nuclear magnetic resonance, J. Chem. Phys. 101 (1994) 1805–1812.
[62] W.G. Hu, K. Schmidt-Rohr, Polymer ultradrawability: the crucial role of α-relaxation chain mobility in the crystallites, Acta Polym. 50 (1999) 271–285.
[63] C. Tang, A. Inomata, Y. Sakai, H. Yokoyama, T. Miyoshi, K. Ito, Effects of chemical modification on the molecular dynamics of complex polyrotaxanes investigated by solid-state NMR, Macromolecules 46 (2013) 6898–6907.
[64] X. Yuan, D. Sperger, E.J. Munson, Investigating miscibility and molecular mobility of nifedipine-PVP amorphous solid dispersions using solid-state NMR spectroscopy, Mol. Pharm. 11 (2014) 329–337.
[65] K.R. Mote, V. Agarwal, P.K. Madhu, Five decades of homonuclear dipolar decoupling in solid-state NMR: status and outlook, Prog. Nucl. Magn. Reson. Spectrosc. 97 (2016) 1–39.
[66] P.K. Madhu, High-resolution solid-state NMR spectroscopy of protons with homonuclear dipolar decoupling schemes under magic-angle spinning, Solid State Nucl. Magn. Reson. 35 (2009) 2–11.
[67] A.M. Jordan, K. Kim, D. Soetrisno, J. Hannah, F.S. Bates, S.A. Jaffer, O. Lhost, C.W. Macosko, Role of crystallization on polyolefin interfaces: an improved outlook for polyolefin blends, Macromolecules 51 (2018) 2506–2516.
[68] K. Ishizuki, D. Aoki, R. Goseki, H. Otsuka, Multicolor mechanochromic polymer blends that can discriminate between stretching and grinding, ACS Macro Lett. 7 (2018) 556–560.
[69] S. Lu, R. Zhang, X. Wang, P. Sun, W. Lv, Q. Liu, N. Jia, Effect of PEO molecular weight on the miscibility and dynamics in epoxy/PEO blends, Euro. Phys. J. E 38 (2015) 1–8.
[70] D. Tian, T. Li, R. Zhang, Q. Wu, T. Chen, P. Sun, A. Ramamoorthy, Conformations and intermolecular interactions in cellulose/silk fibroin blend films: a solid-state NMR perspective, J. Phys. Chem. B 121 (2017) 6108–6116.
[71] T.H. Chen, J.J. Zhu, B.H. Li, S.Y. Guo, Z.Y. Yuan, P.C. Sun, D.T. Ding, A.C. Shi, Exfoliation of organo-clay in telechelic liquid polybutadiene rubber, Macromolecules 38 (2005) 4030–4033.
[72] T. Gopinath, S.E.D. Nelson, G. Veglia, 1H-detected MAS solid-state NMR experiments enable the simultaneous mapping of rigid and dynamic domains of membrane proteins, J. Magn. Reson. 285 (2017) 101–107.
[73] T. Gopinath, G. Veglia, 3D DUMAS: Simultaneous acquisition of three-dimensional magic angle spinning solid-state NMR experiments of proteins, J. Magn. Reson. 220 (2012) 79–84.
[74] T. Gopinath, G. Veglia, Dual acquisition magic-angle spinning solid-state NMR-spectroscopy: simultaneous acquisition of multidimensional spectra of biomacromolecules, Angew. Chem. Int. Ed. 51 (2012) 2731–2735.
[75] K. Sharma, P.K. Madhu, K.R. Mote, A suite of pulse sequences based on multiple sequential acquisitions at one and two radiofrequency channels for solid-state magic-angle spinning NMR studies of proteins, J. Biomol. NMR 65 (2016) 127–141.
[76] C. Martineau, F. Decker, F. Engelke, F. Taulelle, Parallelizing acquisitions of solid-state NMR spectra with multi-channel probe and multi-receivers: applications to nanoporous solids, Solid State Nucl. Magn. Reson. 55–56 (2013) 48–53.
[77] Ē. Kupče, K.R. Mote, P.K. Madhu, Experiments with direct detection of multiple FIDs, J. Magn. Reson. 304 (2019) 16–34.
[78] R. Zhang, Y. Chen, N. Rodriguez-Hornedo, A. Ramamoorthy, Enhancing NMR sensitivity of natural-abundance low-γ nuclei by ultrafast magic-angle-spinning solid-state NMR spectroscopy, ChemPhysChem 17 (2016) 2962–2966.
[79] S.A. Kotler, J.R. Brender, S. Vivekanandan, Y. Suzuki, K. Yamamoto, M. Monette, J. Krishnamoorthy, P. Walsh, M. Cauble, M.M.B. Holl, E.N.G. Marsh, A. Ramamoorthy, High-resolution NMR characterization of low abundance oligomers of amyloid-β without purification, Sci. Rep. 5 (2015) 11811.
[80] X. Lu, C. Huang, M.B. Lowinger, F. Yang, W. Xu, C.D. Brown, D. Hesk, A. Koynov, L. Schenck, Y. Su, Molecular interactions in posaconazole amorphous solid dispersions from two-dimensional solid-state NMR spectroscopy, Mol. Pharm. 16 (2019) 2579–2589.
[81] Y. Su, A.J. Waring, P. Ruchala, M. Hong, Membrane-bound dynamic nature of an arginine-rich cell-penetrating peptide, the protein transduction domain of HIV TAT, from solid-state NMR, Biochemistry 49 (2010) 6009–6020.